PHYSICAL REVIEW C **88**, 031304(R) (2013)

Quadrupole moments of coexisting collective shapes at high spin in ^{154}Er

J. P. Revill,[1] E. S. Paul,[1] X. Wang,[2] M. A. Riley,[2] J. Simpson,[3] R. V. F. Janssens,[4] J. Ollier,[3] A. J. Boston,[1] M. P. Carpenter,[4] C. J. Chiara,[4,5] C. R. Hoffman,[4] F. G. Kondev,[6] T. Lauritsen,[4] P. J. Nolan,[1] J. M. Rees,[1] S. V. Rigby,[1] C. Unsworth,[1] S. Zhu,[4] and I. Ragnarsson[7]

[1]*Oliver Lodge Laboratory, University of Liverpool, Liverpool L69 7ZE, United Kingdom*
[2]*Department of Physics, Florida State University, Tallahassee, Florida 32306, USA*
[3]*STFC Daresbury Laboratory, Daresbury, Warrington WA4 4AD, United Kingdom*
[4]*Physics Division, Argonne National Laboratory, Argonne, Illinois 60439, USA*
[5]*Department of Chemistry and Biochemistry, University of Maryland, College Park, Maryland 20742, USA*
[6]*Nuclear Engineering Division, Argonne National Laboratory, Argonne, Illinois 60439, USA*
[7]*Division of Mathematical Physics, LTH, Lund University, P.O. Box 118, S-22100 Lund, Sweden*

(Received 24 June 2013; published 9 September 2013)

Four high-spin collective bands have been populated in $^{154}_{68}Er_{86}$ via the ^{110}Pd(^{48}Ti, $4n\gamma$)^{154}Er reaction. Average transition quadrupole moments Q_t have been measured for three of the bands by using the Doppler-shift attenuation method. The strongest band has a value of $Q_t = 11.0 \pm 1.0\ e$ b, similar to values found recently for four triaxial strongly deformed (TSD) bands in ^{157,158}Er. The second band has a value of $Q_t = 19.5 \pm 3.2\ e$ b, consistent with a predicted axially symmetric superdeformed (SD) shape, similar in deformation to the ^{152}Dy isotone, and is used as a calibration point. The third, new band has a value of $Q_t = 9.9 \pm 2.2\ e$ b. The results confirm the unexpectedly large Q_t moments for the favored TSD bands in light erbium isotopes.

DOI: 10.1103/PhysRevC.88.031304 PACS number(s): 27.70.+q, 21.10.Re, 23.20.Lv

In nature, the ideal spherical shape is often not realized. For example, due to its rotation, the earth is oblate with its equatorial diameter larger than the pole-to-pole diameter; spherical symmetry is, thus, broken. Further symmetry breaking is evident in triaxial shapes (e.g., a kiwi fruit), which have three spatial principal axes of different lengths and, consequently, no rotational axis of symmetry. In the subatomic world, nonaxial nuclear shapes, described by the triaxiality parameter γ in the polar representation of rotating quadrupole shapes [1], may be stabilized at high spin by shell effects that lead to lower level densities for triaxial shapes [2,3] and by aligned valence particles in high-j anisotropic orbitals [4,5]. The most asymmetric triaxial shape is realized for $\gamma \sim \pm 30^\circ$ or $\sim -90^\circ$. These particular triaxial shapes are equivalent with distinct "long," "short," and "intermediate" principal axes; it is only the axis about which the nucleus rotates that is different. For $0^\circ < \gamma < 60^\circ$, the nucleus rotates about the short axis, for $-60^\circ < \gamma < 0^\circ$, the nucleus rotates about the intermediate one, and for $-120^\circ < \gamma < -60^\circ$, the nucleus rotates about the long axis. The largest moment of inertia is achieved for $0^\circ < \gamma < 60^\circ$ and, hence, classically, a triaxial body minimizes its energy for such motion. However, for the nucleus, a quantum system, strong coupling between collective and single-particle angular momenta can determine the overall shape and can influence the way in which it rotates, or indeed, precesses (wobbles) [6]. Wobbling is a unique characteristic of triaxial shapes [7].

In this Rapid Communication, the measurement of quadrupole moments of three high-spin bands in ^{154}Er is reported. Two of the bands were identified previously [8,9]. For these two bands, comparison of experimental moment-of-inertia properties with Woods-Saxon cranking calculations suggested that one band is associated with a triaxial strongly deformed (TSD) nuclear shape, whereas, the other represents an axial superdeformed (SD) nuclear shape [9]. Such shape coexistence at high spin was previously predicted for ^{154}Er in Refs. [10,11]. Recent work on corresponding TSD bands in ^{157,158}Er [12,13] yielded unexpectedly large experimental quadrupole moments (at $I \sim 30$–50), at variance with theoretical predictions, see Ref. [3]. Although configurations could be found in the calculations with appropriate values of the transition quadrupole moment Q_t, they were not the favored ones, lying $\sim$1 MeV higher in energy within the $I \sim 30$–50 range than other less deformed, but triaxial, configurations. Only at spin values beyond 60 $\hbar$ did these large Q_t configurations become the favored TSD shape. A similar conclusion was found when considering self-consistent tilted-axis cranking [14]. The coexistence of TSD and axial SD shapes at high spin in ^{154}Er, therefore, provides a golden opportunity to explore this puzzling discrepancy between data and calculations and, indeed, to calibrate the extracted quadrupole moments for TSD bands in the light erbium isotopes.

An experiment was carried out at Argonne National Laboratory. A 215-MeV ^{48}Ti beam was delivered by the ATLAS facility to bombard a 1-mg/cm^2 ^{110}Pd target backed by a 10-mg/cm^2 layer of ^{197}Au, which produces ^{154}Er nuclei via the ^{110}Pd(^{48}Ti, $4n$) reaction. An additional 0.07-mg/cm^2 layer of Al between the Pd and the Au was used to prevent the migration of the target material into the backing. The emitted γ rays were collected by the Gammasphere spectrometer [15,16], which consists of 101 Compton-suppressed HPGe detectors. Approximately 3.9×10^9 events of folds four or higher were collected. Additional data, which composed $\sim 8 \times 10^8$ events of folds three or above, were recorded by using a stack of two thin self-supporting targets with a total thickness of 1 mg/cm^2.

In addition to the TSD and SD bands (bands 1 and 2), two new bands with high moments of inertia were found in ^{154}Er (bands 3 and 4), and the SD band of ^{151}Dy [17] was populated

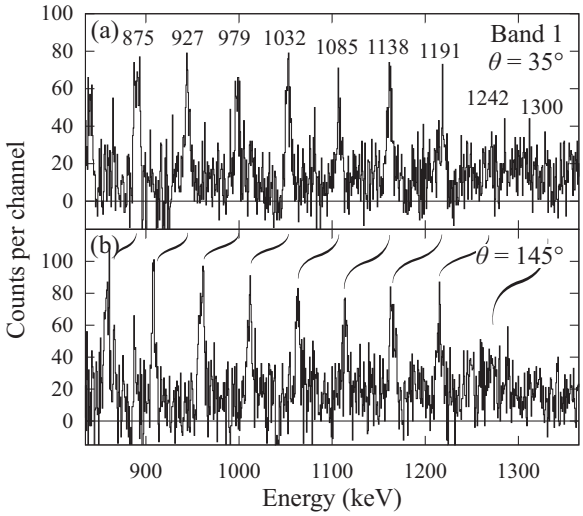

FIG. 1. Angle-dependent, triple-gated, and background-subtracted coincidence spectra for band 1 of ^{154}Er. In-band transitions are labeled with their unshifted energies in keV.

as well through the $\alpha 3n$ channel. γ-ray spectra for the four bands of ^{154}Er are seen in Figs. 1 and 2. The intensity of band 1 is estimated to be 0.6% relative to the ^{154}Er channel intensity in agreement with previous measurements [8,9]. The intensity of band 2 is approximately a factor of 2 smaller than that of band 1, whereas, the intensities of bands 3 and 4 are another factor of 2 weaker. The in-band transitions are assumed to be of collective stretched-$E2$ character. The four

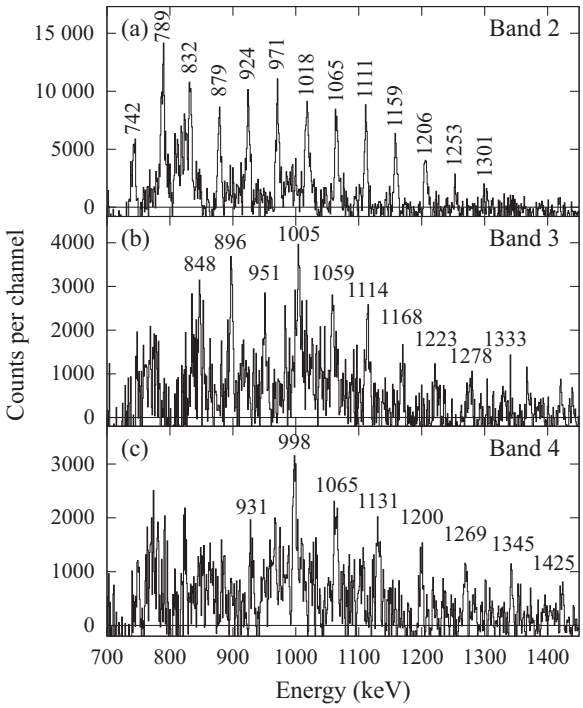

FIG. 2. Double-gated background-subtracted coincidence spectra for (a) band 2, (b) band 3, and (c) band 4 of ^{154}Er. A Doppler correction with an average value of v/c has been applied. Transitions are labeled with their energies in keV.

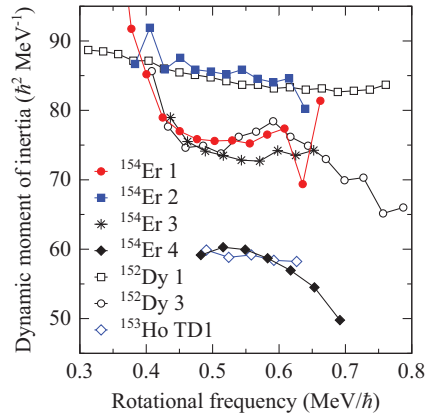

FIG. 3. (Color online) Dynamic moments of inertia for bands in ^{154}Er and $N = 86$ isotones ^{152}Dy and ^{153}Ho [19–21].

bands clearly populate yrast states in ^{154}Er [18] up to 25^- in agreement with previous work for bands 1 and 2 [8,9]. In Fig. 1, angle-dependent spectra are given for band 1, whereas, in Fig. 2, a Doppler correction with an average value of v/c has been applied to produce a spectrum summed over all angles for bands 2–4. A gatelist of the relevant band members was used in each case.

Dynamic moments of inertia $\mathcal{J}^{(2)} \approx dI/d\omega$ for the four collective bands in ^{154}Er are compared in Fig. 3 with bands in the $N = 86$ isotones ^{152}Dy and ^{153}Ho [19,20]. (Note that, in each of these $N = 86$ isotones, the yrast line up to $I \sim 45$ is dominated by oblate or near-oblate excitations with small or no collectivity.) It can be seen that ^{154}Er band 2 has a moment of inertia around $85\hbar^2$ MeV^{-1}, similar to the SD band in ^{152}Dy [19] (labeled ^{152}Dy 1 in Fig. 3), whereas, ^{154}Er bands 1 and 3 have values around $75\hbar^2$ MeV^{-1}, similar to a proposed TSD band in ^{152}Dy [20] (labeled ^{152}Dy 3 in Fig. 3) and others in ^{158}Er [12]. The moment of inertia of ^{154}Er band 4 is lower, around $60\hbar^2$ MeV^{-1}, but similar to other proposed triaxially deformed (TD) bands in ^{152}Dy and ^{153}Ho [20,21] (labeled ^{153}Ho TD1 in Fig. 3). The different average values of the moments of inertia give an indication of the presence of three distinct shapes with different quadrupole deformations.

Although the moments of inertia provide an insight into possible relative deformations of the bands, definitive conclusions can only be drawn from measured quadrupole moments. Hence, the Doppler-shift attenuation method [22] was used to measure mean nuclear level lifetimes and to extract average transition quadrupole moments Q_t for three of the bands in ^{154}Er. Angle-dependent spectra for bands 1–3 in ^{154}Er were generated. The mean recoil velocity in the middle of the ^{110}Pd target layer was measured to be $v_0 = 0.0286c$. The fractional Doppler shift $F(\tau)$ and associated errors were subsequently extracted from linear fits of the energy shifts as a function of detector angle θ. The approach employed is similar to that described in Refs. [23,24]. The resulting measured $F(\tau)$ values are presented in Fig. 4. Fitted $F(\tau)$ curves for constant in-band Q_t and equal side-feeding Q_{sf} quadrupole moments are also provided. The curves were obtained by using the code package MLIFETIME [25] combined with stopping powers obtained from the SRIM 2008 package [26].

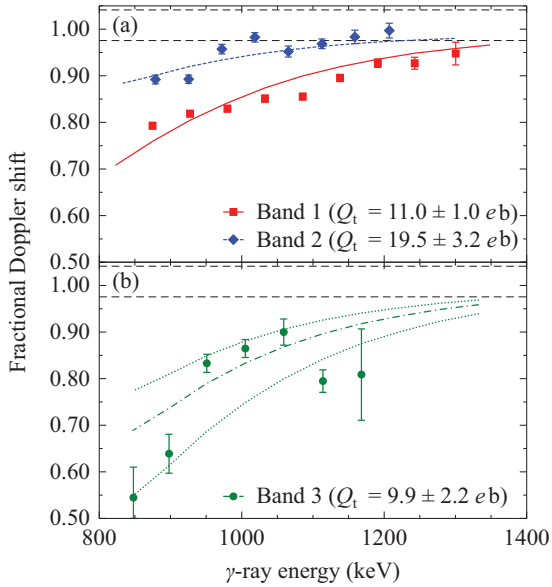

FIG. 4. (Color online) Measured fractional Doppler-shift values $F(\tau)$ shown as a function of γ-ray energy together with best fit curves for (a) bands 1 and 2 and (b) band 3 in ^{154}Er. In (b), curves are also shown for the quoted error on Q_t. The two horizontal dashed lines indicate the range of initial recoil velocities within the ^{110}Pd target layer.

The quadrupole moment $Q_t = 19.5 \pm 3.2\ e$ b, extracted for ^{154}Er band 2 is similar to that of the SD band in the ^{152}Dy isotone [17]. Furthermore, a similar value was also obtained from the present data for the SD band of ^{151}Dy, which is also consistent with a previous measurement for that nucleus [17]. The quadrupole moments $Q_t = 11.0 \pm 1.0$ and $Q_t = 9.9 \pm 2.2\ e$ b, extracted for ^{154}Er bands 1 and 3, respectively, are similar to the values obtained for the four TSD bands in ^{157,158}Er [12]. It was not possible to produce reliable angle-dependent spectra for the weaker ^{154}Er band 4. It is, however, apparent that a number of distinct collective shapes coexist at high spin in ^{154}Er.

In order to address the high-spin behavior of ^{154}Er, theoretical calculations have been performed in the framework of the configuration-dependent cranked Nilsson-Strutinsky (CNS) method without pairing [27,28]. In the present calculations, the formalism presented in Ref. [29] has been used with κ and μ parameters that define the $\boldsymbol{\ell} \cdot \boldsymbol{s}$ and $\boldsymbol{\ell}^2$ strengths of the modified oscillator potential, taken from Ref. [30]. Typical potential-energy surface plots, which are representative of all four parity-signature combinations, are shown in Fig. 5. They are, in general, consistent with the total Routhian surfaces presented in Ref. [9] with four competing minima at high spin $I \sim 60$, i.e., SD at $\varepsilon_2 \sim 0.6$, $\gamma \sim 0°$, triaxial at $\varepsilon_2 \sim 0.35$, $\gamma \sim \pm 15°$, and (close to) noncollective at $\gamma \sim 60°$. In terms of high-j orbitals, the SD minimum, which becomes yrast at $I \sim 60$, is based on the configuration $\pi\{(i_{13/2})^4\} \otimes \nu\{(i_{13/2})^8(j_{15/2})^2\}$ and has a predicted moment $Q_t \sim 20\ e$ b. CNS calculations suggest that the high-j configuration of ^{154}Er is the same as that for the lowest SD band in ^{152}Dy with the additional protons placed in $\mathcal{N} = 4$ and 5 orbitals based on the [411]3/2, [413]5/2 and [530]1/2, [532]3/2 Nilsson orbitals, respectively.

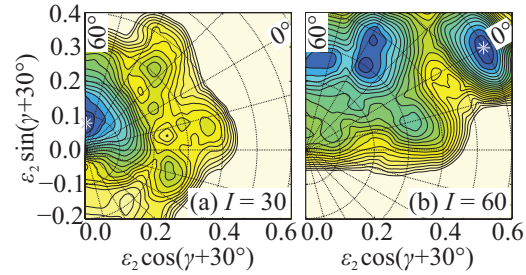

FIG. 5. (Color online) Total energy surfaces for ^{154}Er at (a) $I = 30$ and (b) $I = 60$ for $(\pi, \alpha) = (+, 0)$. The contour line separation is 0.25 MeV with the last contour line approximately 5 MeV above the minimum, which is marked with a star.

In general, the most reliable interpretation of the SD bands has been obtained by comparing their relative properties. One example is in terms of effective alignments (i_{eff}), see e.g., Refs. [31,32]. Therefore, a comparison of ^{154}Er band 2 with the lowest SD band in ^{152}Dy [33] has been carried out. The latter band is well understood since it is connected to the normal-deformed states so that its spin values are known [34]. Effective alignments of calculated configurations in ^{154}Er relative to the ^{152}Dy yrast SD configuration are displayed in Fig. 6. It is seen that two valence protons placed in $\mathcal{N} = 5$ orbitals contribute with an alignment of approximately $2\hbar$, whereas, approximately $1\hbar$ is gained if they are placed in $\mathcal{N} = 4$ orbitals. This analysis and the fact that, for the ^{152}Dy band, the spins are known limit the lowest spin of band 2 to be close to $I = 30$. Indeed, the best agreement between experiment and calculations is obtained if the "band-head" spin of band 2 in ^{154}Er is fixed at $I_0 = 32$ and the band is assigned to the configuration with the two additional protons in the $\mathcal{N} = 5$ orbitals. However, this implies that ^{154}Er band 2 has spin values $6\hbar$ higher than the original suggestion of $26\hbar$ proposed in Ref. [9].

Bands 1 and 3 in ^{154}Er have similar moments of inertia (Fig. 3). With measured transitional quadrupole moments of

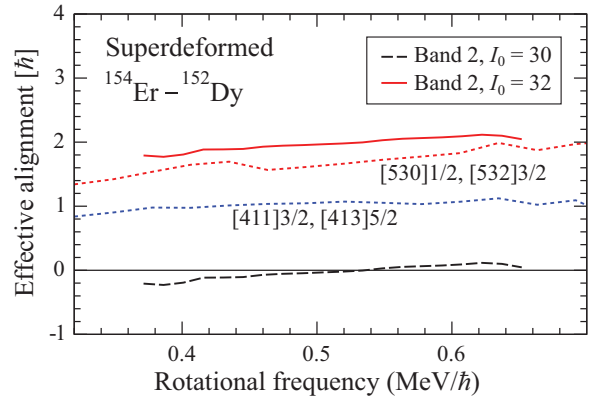

FIG. 6. (Color online) Observed effective alignments when band 2 in ^{154}Er is compared with the yrast SD band of ^{152}Dy. Two curves are shown where the spin of the lowest state in ^{154}Er is assumed to be 30 (dashed curve) and $32\hbar$ (solid curve). These curves are compared with calculated values (dotted curve) when the two valence protons are in the two signatures of the lowest $\mathcal{N} = 4$ and 5 orbitals, respectively.

$Q_t = 10$ to 11 e b, these bands could be assigned to TSD configurations of the type shown in Fig. 7. These configurations are labeled relative to a $^{146}_{64}Gd_{82}$ closed core, i.e.,

$$\pi(h_{11/2})^{p_1}(h_{9/2}f_{7/2})^{p_2}(i_{13/2})^{p_3}\cdots\nu(\mathcal{N}=4)^{-n_1} \times (h_{11/2})^{-n_2}(i_{13/2})^{n_3},$$

which specifies the number of particles and holes in orbitals of different characters outside the core. The number of protons in $\mathcal{N} = 4$ orbitals and neutrons in $h_{9/2}f_{7/2}$ states is then fixed from the particle numbers $Z = 68$ and $N = 86$, respectively. The configurations will be given in the shorthand notation $[p_1(p_2p_3), (n_1n_2)n_3]$. The calculations predict that positive-γ configurations are lowest in energy at high spin (see Fig. 5) with $\varepsilon_2 \approx 0.35$, $\gamma \approx 20^\circ$. The negative γ minimum (rotation around the intermediate axis) at $\varepsilon_2 \approx 0.35$, $\gamma \approx -15^\circ$ is another possibility.

For positive-γ deformations, the favored proton configuration for $Z = 68$ is [6(21)] in a large frequency and deformation range. If it is combined with a neutron configuration with as many $\mathcal{N} = 4$ holes and $\mathcal{N} = 6$ particles as possible, e.g., [(42)4], the largest possible Q_t for such configurations is obtained, namely, 8.3 e b. This is still lower than measured. In the cranked relativistic mean-field (CRMF) theory [35], for a configuration with the same number of protons and neutrons in the $\mathcal{N} = 6$ orbitals as the CNS configuration, a value of $Q_t \approx 9$ e b is obtained. Note that the definition of γ is different in the present CNS calculations and in CRMF- or Skyrme-type calculations, see Ref. [36]. If the $\mathcal{N} = 6$ proton shell was lower in energy, configurations with two $i_{13/2}$ protons would become more competitive. For example, the [6(22),(42)4] configuration included in Fig. 7 has a predicted Q_t value of 9.7 e b, which is closer to the measured one. However, similar to band 2, the spins of band 1 need to be 4–6$\hbar$ higher than previously suggested in Refs. [8,9] for this interpretation.

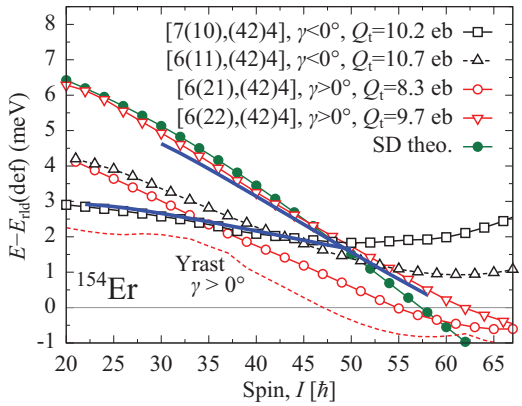

FIG. 7. (Color online) Calculated TSD configurations at $\gamma < 0^\circ$ and $\gamma > 0^\circ$, which might be assigned to band 1. Values of Q_t at $I = 40$ are specified for each configuration. It is also demonstrated how a good agreement between the observed band 1, drawn by the solid line, and the calculated bands can be obtained in the two extreme cases of the $\gamma < 0^\circ$ [7(10),(42)4] configuration and the $\gamma > 0^\circ$ [6(22),(42)4] configuration but with very different values of the band-head spin 22$\hbar$ and 30$\hbar$, respectively. The dashed line labeled "Yrast, $\gamma > 0^\circ$" corresponds to the lowest energy, independent of signature and parity, for the minima with $\gamma \sim 15^\circ$–30°, $\varepsilon_2 \sim 0.3$–0.4. The calculated lowest-energy SD configuration with $\varepsilon_2 = 0.6$ is also included.

The configurations in the negative-γ minimum are low in energy at low spin as exemplified by the [7(10),(42)4] and [6(11),(42)4] configurations in Fig. 7. They are, however, higher in energy than the positive-γ configurations for $I > 55$. Their predicted Q_t values of just over 10 e b match the experimental values extracted for ^{154}Er bands 1 and 3. A recent analysis of relative alignments in TSD bands in ^{158}Er and neighboring nuclei [37] concluded that negative-γ shapes (rotation about the intermediate axis) best describe their general properties. However, as seen in Fig. 7, a rather low band-head spin of $I_0 = 22$ is required to best describe the ^{154}Er data. It is noteworthy that this is consistent with the observed relative intensities of the SD and TSD bands, which differ by a factor of 2. In contrast, in Fig. 7, where the SD and suggested positive-γ TSD [6(22),(42)4] configuration track each other closely, one would expect equal population.

When comparing the positive- and negative-γ minima, it is interesting to note that a tilted-axis-cranking approach has recently been applied to the TSD bands near $A = 160$ [14]. For ^{158}Er, specifically, these results indicate that, if a true energy minimum occurs for shapes with positive γ, the negative-γ shape only represents a saddle point when the axis of rotation is allowed to change direction. Of course, this requires that there be a positive-γ minimum which is lower than the negative-γ one for the specific configuration. This is the case for the [6(11),(42)4] configuration but not for the [7(10),(42)4] one where the negative-γ minimum is calculated lowest in energy up to $I \approx 50$.

Although a quadrupole moment could not be extracted for band 4, it has a lower moment of inertia than bands 1–3 (Fig. 3). Similar bands have been observed in neighboring nuclei with $A = 152$, 153 [20,21]. With the observation of the first band of this kind [38], it was concluded [39] that it might be assigned to either an axial configuration ($\varepsilon_2 \sim 0.2$ with two $\nu h_{11/2}$ holes) or a triaxial configuration ($\varepsilon_2 \sim 0.3$, $\gamma \sim \pm 15^\circ$ with two $\nu h_{11/2}$ and two $\mathcal{N} = 4$ holes).

To summarize, relative quadrupole moments have been extracted for the two known high-spin collective bands in ^{154}Er in addition to a third newly identified band. The results for bands 1 and 3 ($Q_t \approx 10$ to 11 e b) and band 2 ($Q_t \approx 20$ e b) are consistent with coexisting TSD and axial SD nuclear shapes in this nucleus at high spin as originally proposed in Ref. [9]. Although a quadrupole moment could not be extracted for band 4, its lower moment of inertia suggests the presence of yet another competing less-deformed collective shape in ^{154}Er at high spin. A comparison with the SD band in ^{152}Dy indicates that the spin values of band 2 in ^{154}Er are considerably higher than previous suggested [9]. Furthermore, similar to high-spin bands in ^{157,158}Er [12], the measured Q_t moments for bands 1 and 3 are significantly larger than the value predicted for favored CNS configurations. If these bands were to be assigned to large-deformation TSD configurations with $\gamma > 0^\circ$, a similar increase in spin values is required as for band 2, a situation similar to that suggested in ^{158}Er [14,40]. These results point to the need for further measurements in this region of triaxial strongly deformed structures to provide

more precise Q_t, excitation energy, and spin values for these bands in order to solve this intriguing puzzle.

The staff at Argonne National Laboratory are thanked for their excellent support. Valuable discussions with A. V. Afanasjev and W. Nazarewicz are acknowledged. This work was supported, in part, by the US National Science Foundation under Grants No. PHY04-51120 and No. PHY07-54674, the US Department of Energy, Office of Nuclear Physics, under Grant No. DE-FG02-94ER40834 and Contracts No. DE-AC02-06CH11357 and No. DE-FG02-95ER40934, the UK Science and Technology Facilities Council, the Swedish Science Research Council, as well as by the State of Florida.

[1] G. Andersson *et al.*, Nucl. Phys. **A268**, 205 (1976).
[2] S. E. Larsson, P. Möller, and S. G. Nilsson, Phys. Scr. A **10**, 53 (1974).
[3] E. S. Paul *et al.*, Phys. Rev. Lett. **98**, 012501 (2007).
[4] S. Frauendorf and F. R. May, Phys. Lett. **125B**, 245 (1983).
[5] M. Matev, A. V. Afanasjev, J. Dobaczewski, G. A. Lalazissis, and W. Nazarewicz, Phys. Rev. C **76**, 034304 (2007).
[6] S. W. Ødegård *et al.*, Phys. Rev. Lett. **86**, 5866 (2001).
[7] A. Bohr and B. R. Mottelson, *Nuclear Structure* (Benjamin, New York, 1975), Vol. II.
[8] L. A. Bernstein *et al.*, Phys. Rev. C **52**, R1171 (1995).
[9] K. Lagergren *et al.*, Phys. Rev. Lett. **87**, 022502 (2001).
[10] F. A. Beck *et al.*, Z. Phys. A **319**, 119 (1984).
[11] J. Dudek and W. Nazarewicz, Phys. Rev. C **31**, 298 (1985).
[12] X. Wang *et al.*, Phys. Lett. B **702**, 127 (2011).
[13] X. Wang *et al.*, J. Phys.: Conf. Ser. **381**, 012065 (2012).
[14] Y. Shi, J. Dobaczewski, S. Frauendorf, W. Nazarewicz, J. C. Pei, F. R. Xu, and N. Nikolov, Phys. Rev. Lett. **108**, 092501 (2012).
[15] I. Y. Lee, Nucl. Phys. **A520**, 641c (1990).
[16] R. V. F. Janssens and F. S. Stephens, Nucl. Phys. News **6**, 9 (1996).
[17] D. Nisius *et al.*, Phys. Lett. B **392**, 18 (1997).
[18] C. Schück, M. A. Deleplanque, R. M. Diamond, F. S. Stephens, and J. Dudek, Nucl. Phys. **A496**, 385 (1989).
[19] P. J. Dagnall *et al.*, Phys. Lett. B **335**, 313 (1994).
[20] D. E. Appelbe *et al.*, Phys. Rev. C **66**, 044305 (2002).
[21] M. B. Smith *et al.*, Phys. Rev. C **61**, 034314 (2000).
[22] S. Devons, G. Manning, and D. S. P. Bunbury, Proc. Phys. Soc., London, Sect. A **68**, 18 (1955).
[23] X. Wang *et al.*, Phys. Rev. C **75**, 064315 (2007).
[24] X. Wang, Ph.D. thesis, University of Notre Dame, 2007.
[25] E. F. Moore (private communication).
[26] J. F. Ziegler, J. P. Biersack, and U. Littmark, *The Stopping and Range of Ions in Solids* (Pergamon, New York, 1985).
[27] A. V. Afanasjev, D. B. Fossan, G. J. Lane, and I. Ragnarsson, Phys. Rep. **322**, 1 (1999).
[28] T. Bengtsson and I. Ragnarsson, Nucl. Phys. **A436**, 14 (1985).
[29] B. G. Carlsson and I. Ragnarsson, Phys. Rev. C **74**, 011302(R) (2006).
[30] T. Bengtsson, Nucl. Phys. **A512**, 124 (1990).
[31] B. Haas *et al.*, Nucl. Phys. **A561**, 251 (1993).
[32] A. V. Afanasjev, G. A. Lalazissis, and P. Ring, Nucl. Phys. **A634**, 395 (1998).
[33] P. J. Twin *et al.*, Phys. Rev. Lett. **57**, 811 (1986).
[34] T. Lauritsen *et al.*, Phys. Rev. Lett. **88**, 042501 (2002).
[35] A. V. Afanasjev and P. Ring, Nucl. Phys. **A654**, 647c (1999).
[36] Y. R. Shimizu, T. Shoji, and M. Matsuzaki, Phys. Rev. C **77**, 024319 (2008).
[37] A. Kardan, I. Ragnarsson, H. Miri-Hakimabad, and L. Rafat-Motevali, Phys. Rev. C **86**, 014309 (2012).
[38] B. M. Nyakó, J. R. Cresswell, P. D. Forsyth, D. Howe, P. J. Nolan, M. A. Riley, J. F. Sharpey-Schafer, J. Simpson, N. J. Ward, and P. J. Twin, Phys. Rev. Lett. **52**, 507 (1984).
[39] I. Ragnarsson and S. Åberg, Phys. Lett. B **180**, 191 (1986).
[40] A. V. Afanasjev, Y. Shi, and W. Nazarewicz, Phys. Rev. C **86**, 031304(R) (2012).